Heterogeneous Catalysis

CO Oxidation Catalyzed by Supported Gold: Cooperation between Gold and Nanocrystalline Rare-Earth Supports Forms Reactive Surface Superoxide and Peroxide Species**

*Javier Guzman, Silvio Carrettin, Juan C. Fierro-Gonzalez, Yalin Hao, Bruce C. Gates, and Avelino Corma**

Novel catalysts for environmental and energy-related conversions are increasingly emerging from rational design based on the understanding of relationships between structure at the molecular level and catalyst performance. Gold that is highly dispersed on metal oxides has surprisingly been found to be an active and selective catalyst for numerous reactions,[1,2] including CO oxidation.[3] Contradictory hypotheses have been advanced to account for the CO oxidation activity,[4–13] and the nature of the active sites and reactive oxygen intermediates remains elusive.[14,15] Herein we show by time-resolved spectroscopy of working catalysts consisting of gold nanoclusters on nanocrystalline CeO_{2-x} that η^1-superoxide and peroxide intermediates are formed at one-electron defect sites at the metal–support interface and oxidize adsorbed CO to CO_2. The reactive oxygen species are not formed on conventionally prepared CeO_2, and their formation on nanocrystalline CeO_{2-x} is enhanced by the presence of the gold. This report is the first that unambiguously identifies and quantifies reactive oxygen species in low-temperature CO oxidation catalysis. The new concept advanced here is the representation of the catalytically active species as a composite that uniquely facilitates the formation of reactive oxygen species at the metal–support interface. The generality of the concept is exemplified by results showing that the nanocrystalline oxide can be either CeO_{2-x} or Y_2O_3.[16] This concept opens new avenues to the design of novel materials with improved activities and selectivities for catalytic oxidation.

We prepared high-surface-area ($S_{BET} = 180\ m^2 g^{-1}$; BET refers to Brunauer, Emmett, and Teller) and thermally stable nanocrystalline CeO_{2-x} with the fluorite structure by self-assembly in a liquid-crystal phase of individual CeO_2 nanoparticles with an average diameter of 5 nm.[17] Calcination of the nanocrystalline CeO_{2-x} at 873 K either in the absence or in the presence of 20 wt% H_2O produced minor changes in the BET surface area ($S_{BET} = 160\ m^2 g^{-1}$). CeO_2 was also prepared by a conventional precipitation–calcination method to facilitate a comparison with the nanocrystalline material and to allow investigation of the influence of the surface structure.[12] Deposition–precipitation of gold on the two supports yielded samples with gold loadings in the range of 0.9–4.6 wt%. These samples were characterized by the following spectroscopic methods as they functioned as catalysts for CO oxidation at steady state in flow reactors: X-ray absorption near edge structure (XANES); extended X-ray absorption fine structure (EXAFS); Raman; IR. Each of the samples catalyzed CO oxidation but gold supported on conventional CeO_2 was much less active than that on the nanocrystalline support. The spectra provide information that characterizes the oxidation state(s) and structure of the gold atoms as well as reactive oxygen species derived from the support and reactants.

Highly active gold supported on nanocrystalline CeO_{2-x} was characterized during treatment in He and during catalytic CO oxidation at room temperature; in each case, the EXAFS first-shell Au–Au coordination number $N_{Au\text{-}Au}$ was close to 4 (Table 1), thus indicating the presence of small gold nanoclusters. The absence of higher-shell Au–Au contributions confirms that the nanoclusters did not aggregate during catalysis. Time-resolved XANES spectra (see Supporting Information) indicate cationic gold clusters in the catalyst, which were stable during CO oxidation and this result is consistent with those that show cationic gold clusters in other supported catalysts.[4,5,12]) EXAFS contributions from Au–O at a distance of approximately 2.1 Å demonstrate covalent bonding between gold atoms in the supported clusters and oxygen atoms of the support,[18] and Au–O contributions for longer distances (3.5 Å) indicate nonbonding interactions of gold clusters with oxygen of the support surface (Table 1).

The data that represent the family of samples show a striking correlation: the catalytic activity of nanocrystalline CeO_{2-x}-supported gold clusters increases approximately in proportion to the EXAFS coordination number that represents the Au–O contribution for longer distances (Figure 1). This result indicates the participation of oxygen species at the support surface in CO oxidation. Bolstering this inference, IR spectra recorded for the sample treated with CO in the absence of O_2 indicate formation of CO_2 (see Supporting Information). Thus, the results indicate that nanocrystalline CeO_{2-x} supplies reactive oxygen to the active gold species in CO oxidation, which is consistent with the idea of CeO_2 acting as an oxygen reservoir by releasing and taking up oxygen through redox processes that involve the Ce^{4+}/Ce^{3+} couple.[6] The correlation between catalytic activity and the number of oxygen atoms surrounding—but not bonded to—the gold

[*] Dr. J. Guzman, Dr. S. Carrettin, Prof. Dr. A. Corma
Instituto de Tecnología Química
UPV-CSIC
Universidad Politécnica de Valencia
Avda. de los Naranjos s/n, Valencia 46022 (Spain)
Fax: (+34) 96-387-7809
E-mail: acorma@itq.upv.es
J. C. Fierro-Gonzalez, Y. Hao, Prof. Dr. B. C. Gates
Department of Chemical Engineering and Materials Science
University of California Davis
One Shields Ave.
Davis, CA 95616 (USA)

[**] We thank CICYT (MAT 2003-07945-C02-01), the Auricat European Union network (HPRN-CT-2002-00174), the US National Science Foundation (CTS-0121619; JCF-G), and the US Department of Energy (FG02-04ER15513; YH) for financial support. We also thank the NSLS (supported by the US Department of Energy, DE-AC02-98CH10886) for beam time and the staff of the electron microscopy group at UPV.

Supporting information for this article is available on the WWW under http://www.angewandte.org or from the author.

  DOI: 10.1002/ange.200500659

Table 1: Structural parameters characterizing 2.8 wt% gold on CeO_2 before and during CO oxidation catalysis.[a]

Support	Conditions	$N_{Au\text{-}Au}$	$R_{Au\text{-}Au}$ [Å]	$N_{Au\text{-}O_s}$[b]	$R_{Au\text{-}O_s}$ [Å]	$N_{Au\text{-}O_i}$[c]	$R_{Au\text{-}O_i}$ [Å]	$N_{Au\text{-}C}$	$R_{Au\text{-}C}$ [Å]
conventional CeO_2	He[d]	6.2	2.82						
	catalysis[e]	6.2	2.82						
nanostructured CeO_2	He[d]	4.1	2.84	1.0	2.02	1.3	3.66		
	catalysis[e]	4.1	2.83	1.5	2.06	1.0	3.51	0.2	1.93

[a] N: EXAFS coordination number (error approximately ±10% for metal–metal contributions and ±20% for metal–oxygen contributions); R: EXAFS interatomic distance (error approximately ±1%). [b] $N_{Au\text{-}O_s}$: for shorter Au–$O_{support}$ distance. [c] $N_{Au\text{-}O_i}$: for longer Au–$O_{support}$ distance. [d] He flow of 30 mL min^{-1} at 760 Torr and 298 K. [e] Reaction conditions: 298 K (molar ratio CO/air/He = 0.2:19.8:80.0) and an inverse space velocity of 94 $g_{cat}\,h\,mol_{CO}^{-1}$.

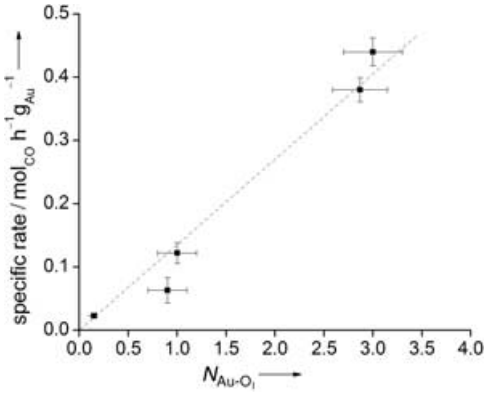

Figure 1. Catalytic activity as a function of the EXAFS coordination number of Au–O_i during CO oxidation catalyzed by gold supported on nanoparticulated CeO_2.

clusters implies that these species are involved in the catalysis, possibly as reactive intermediates that are continuously regenerated by reaction of the surface with O_2.

In contrast, the EXAFS data that characterize gold clusters supported on conventional CeO_2 (which was barely active as a catalyst under the same conditions) do not indicate any Au–O contributions distinguishable above the noise.[19,20] We attribute the near absence of catalytic activity of gold species on the conventional support to the lack of oxygen atoms at the cluster–support interface that can interact fruitfully with the gold atoms. Consistent with this interpretation, we did not detect CO_2 during IR experiments when CO alone was brought in contact with the sample. Furthermore, the differences in catalytic activity between the gold catalysts prepared with conventional and nanocrystalline supports cannot be associated with effects from the different size of the gold particles because the two catalysts have similar distributions of particle size (with an average diameter of about 3–4 nm; see TEM images in the Supporting Information).

To elucidate the nature of the reactive oxygen species on the nanocrystalline support that interact with the gold clusters, we recorded Raman spectra during the room-temperature adsorption of O_2 on CeO_{2-x} alone and on the sample consisting of gold on nanocrystalline CeO_{2-x}; the samples were subsequently exposed to 10% CO in He (Figure 2).

The precise identity of the reactive oxygen species on supported metal catalysts remains to be clarified, although various types of oxygen species have been characterized on cerium oxide.[21] Our results contribute to the understanding of these species and give evidence of a correlation that connects the concentration of reactive oxygen species, their rate of consumption, and the catalytic rate of formation of CO_2 on our catalyst. The spectrum that characterizes the products of O_2 adsorption on nanocrystalline CeO_{2-x} presents bands at 1123, 964, 871, and 831 cm^{-1}, which, on the basis of published data,[22–24] are assigned to η^1-superoxide, peroxide at one-electron defect sites, nonplanar bridging peroxide, and η^2-peroxide species, respectively (see Supporting Information). When CO came into contact with this sample, the intensities of the bands of the oxygen species remained constant and no CO oxidation was detected. In contrast, when O_2 was adsorbed on the gold supported on nanocrystalline CeO_{2-x}

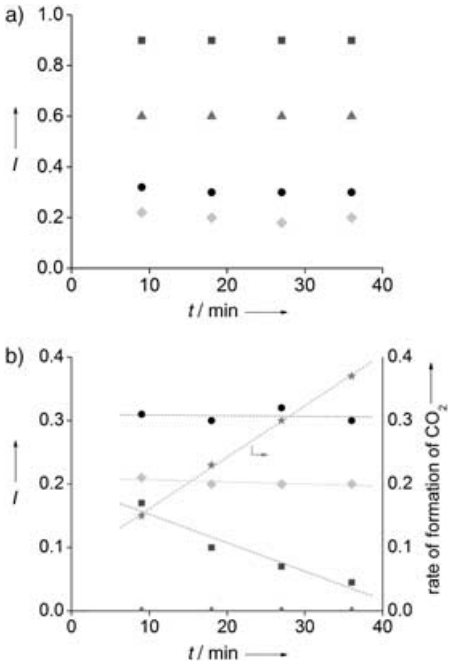

Figure 2. Raman spectra characterizing the formation and reactivity of oxygen species on Au supported on nanostructured CeO_2. Operating conditions were 298 K and 760 Torr: a) adsorption of O_2; b) subsequent exposure to 10% CO in He. The Raman intensities I corresponding to various oxygen species were obtained from the following bands: η^1 superoxide: 1123 cm^{-1} (squares); peroxide at one-electron defect site: 966 cm^{-1} (triangles); nonplanar bridging peroxide: 871 cm^{-1} (circles); and η^2 peroxide: 831 cm^{-1} (diamonds). The rate of formation of CO_2 (stars in (b)) was determined from analysis of the evolved gas phase.

(Figure 2a), the intensities of the bands representing η^1-superoxide and peroxide species at one-electron defect sites were greater than those characterizing the support alone, whereas the intensities of the bands representing nonplanar bridging peroxide and η^2-peroxide species were almost the same. These results indicate a promoting effect of the gold species on the formation of η^1-superoxide and peroxide at one-electron defect sites on the support.

It has been suggested that the presence of gold clusters weakens the bonding of the oxygen species on CeO_2 and facilitates the formation of more reactive species.[6,25] Consistent with this suggestion, we observed that the peroxide species at one-electron defect sites were completely depleted when CO interacted with the sample to form CO_2 (observed in the gas phase); η^1-superoxide species were consumed simultaneously (Figure 2b). There is a correlation between the concentration of each of these species and its rate of consumption and also with the catalytic rate of formation of CO_2 (Figure 2b). In contrast, the concentrations of nonplanar bridging peroxide and η^2-peroxide species remained unchanged (Figure 2b), which indicates that these species do not participate directly in the CO oxidation. Thus, η^1-superoxide and peroxide at one-electron defect sites are identified as reaction intermediates under our conditions, whereas nonplanar bridging peroxide, η^2-peroxide, and molecular oxygen species are either spectators or involved in virtually equilibrated elementary steps in the catalytic cycle.

Consistent with this interpretation, when we performed the same experiments but with a barely active catalyst consisting of gold supported on conventional CeO_2, the only oxygen species observed were nonplanar bridging peroxide adspecies, η^2-peroxide, $O_2^{\delta-}$ $(0<\delta<1)$, and molecular oxygen; no CO_2 formation was detected with this sample under our conditions.

Results of temperature-programmed reduction (TPR) with CO characterizing the catalytically active gold on nanocrystalline CeO_{2-x} confirm the participation of the separate surface oxygen species, which are reactive under various conditions (see Supporting Information). The species reduced at high temperature (820 K) are associated with lattice oxygen, which does not participate in CO oxidation at low temperatures. The oxygen species with maximum CO uptakes at 385 and at 473 K may be attributed to superoxide and peroxide adspecies, respectively. Cyclic TPR experiments (see Supporting Information) demonstrate the regeneration of the active gold sites during reduction and oxidation of the catalyst.

Our results imply a cooperation between gold and the nanocrystalline CeO_{2-x} which promotes the formation of reactive oxygen species (Figure 3). An explanation for the enhanced activity of the catalysts prepared with nanocrystalline CeO_{2-x} is based on the stabilization of cationic gold (indicated by previous reports and supported by our own XANES data)[5,12] and reactive intermediate oxygen species, all at the cluster–support interface; the stabilization is inferred to be caused in part by oxygen vacancies on the nanocrystalline support and facilitated by a synergistic effect associated with the smallness (nanoscale) of both the gold and the support. Consistent with this interpretation, the high surface/grain–boundary area that is characteristic of the CeO_{2-x} nanocrystals is associated with the presence of defects that enhance the electron-transport properties of sintered nanostructured CeO_{2-x} relative to that of bulk CeO_2.[17]

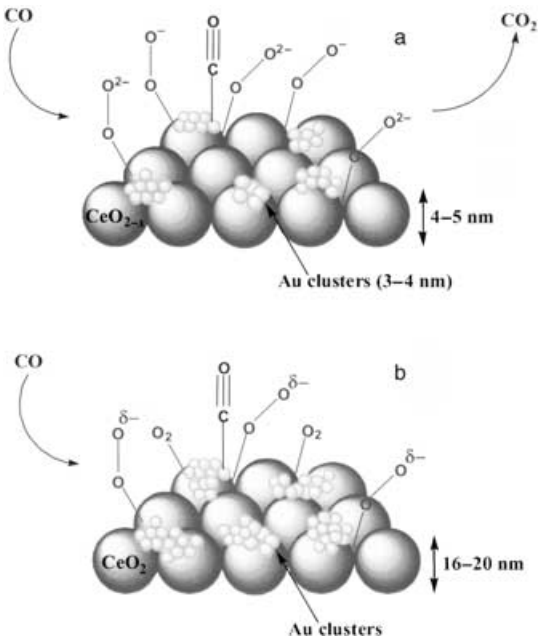

Figure 3. Schematic representation of CO oxidation catalyzed by gold on nanocrystalline (a) and regular (b) CeO_2. a) CO is adsorbed on the gold, whereas the oxygen is supplied through the nanocrystalline CeO_2 support as η^1-superoxide and peroxide adspecies at one-electron defect sites to give CO_2. b) CO is adsorbed on the gold atoms and the oxygen is adsorbed as molecular O_2 and $O_2^{\delta-}$. The size of the atoms is not scaled.

As described in reference [16], a catalyst consisting of gold on Y_2O_3, both nanocrystalline and conventionally prepared, showed similar differences in the catalytic activity as the one studied here; the activity of the catalyst prepared from nanocrystalline Y_2O_3 was shown to be comparable to the activities of the most active supported gold catalysts under similar conditions,[3,13] and the reactive intermediate oxygen species identified by Raman spectroscopy during catalysis were peroxide and superoxide species (see Supporting Information). These results bolster those observed for the CeO_{2-x}-supported samples and demonstrate a general synergistic effect associated with the interfaces between gold and nanocrystalline redox-active supports in promoting the formation of reactive oxygen species that participate in catalytic CO oxidation.

In summary, we have shown a correlation between the catalytic activity of gold supported on nanocrystalline CeO_{2-x} and reactive η^1-superoxide and peroxide species at one-electron defect sites on the support. The formation of reactive oxygen species on the nanocrystalline support is enhanced by the gold. The pattern extends to Y_2O_3 supports, and we infer that the existence of reactive peroxides at gold nanocluster–support interfaces is general and will be useful in the design of novel materials with enhanced catalytic activity and selectivity for oxidation reactions.

Experimental Section

Nanocrystalline CeO_2 and Y_2O_3 were prepared from colloidal dispersions of CeO_2 and Y_2O_3 nanoparticles with average diameters of 5 nm. The conventional CeO_2 support was prepared by precipitation of $Ce(NO_3)_4$; conventional Y_2O_3 was supplied by Nyacol, Inc. Gold was deposited on each support by deposition–precipitation of $HAuCl_4$ with NaOH, as described elsewhere.[12,16] The catalysts were not calcined. The total Au content of each final catalyst was determined by chemical analysis.

Raman spectra, with a resolution of 2 cm^{-1}, were collected with a Renishaw inVia Raman spectrometer equipped with a Leica DMLM microscope and a 514-nm Ar^+ ion laser as an excitation source and with a laser power at the sample of 2.0 mW. Each reported spectrum is the average of 20 scans with an exposure time each of 10 s. O_2 adsorption and CO oxidation experiments were conducted with an in situ cell (Linkam Scientific, THMS 600). The catalysts were pretreated at 323 K under vacuum (10^{-2} Pa) for 1 h before adsorption experiments.

The X-ray absorption spectroscopy experiments were performed at beamline X-18B at the National Synchrotron Light Source, Brookhaven National Laboratory, Upton, NY, USA. The storage ring electron energy was 2.8 GeV and the ring current varied within the range of 110 to 250 mA. Spectra were collected in the fluorescence mode. Higher harmonics in the X-ray beam were minimized by detuning the Si(111) double-crystal monochromator by 20 to 25 % at the Au L_{III} edge (11919 eV). A PIPS detector was used, and each reported spectrum is the average of six scans. Data were recorded during CO oxidation catalysis at 298 K and also with the catalysts in flowing He at atmospheric pressure and 298 K. Catalyst powder (0.3 g) was loaded into a cell/reactor and installed in the flow system at the beamline.

CO oxidation catalysis was carried out at atmospheric pressure in a standard once-through, nearly isothermal tubular packed-bed flow reactor (9 mm in diameter). Total feed flow rate to the reactor was 100 mL (normal temperature and pressure) per minute with a molar ratio of CO/air/He of 0.2:19.8:80.0, with an inverse space velocity of 18.6–94.0 $g_{cat}\,h\,mol_{CO}^{-1}$. The conversions were determined by gas chromatographic analysis of the product stream with an accuracy of about $\pm 5\,\%$. An on-line gas chromatograph (Varian, Star 3400 CX) equipped for column switching (Porapak and molecular sieves) in combination with two-channel detection (with a thermal conductivity detector and a flame-ionization detector) was used to analyze the gas stream.

Received: February 22, 2005
Revised: April 20, 2005
Published online: June 29, 2005

Keywords:
heterogeneous catalysis · cerium · EXAFS spectroscopy · gold · nanostructures

[1] B. Nkosi, M. D. Adams, N. J. Coville, G. J. Hutchings, *J. Catal.* **1991**, *128*, 378 – 386.
[2] a) T. Hayashi, K. Tanaka, M. Haruta, *J. Catal.* **1998**, *178*, 566 – 575; b) E. E. Stangland, K. B. Stavens, R. P. Andres, W. N. Delgass, *J. Catal.* **2000**, *191*, 332 – 386.
[3] M. Haruta, N. Yamada, T. Kobayashi, S. Iilima, *J. Catal.* **1989**, *115*, 301 – 309.
[4] J. Guzman, B. C. Gates, *J. Phys. Chem. B* **2002**, *106*, 7659 – 7665.
[5] J. Guzman, B. C. Gates, *J. Am. Chem. Soc.* **2004**, *126*, 2672 – 2673.
[6] Q. Fu, H. Saltsburg, M. Flytzani-Stephanopoulos, *Science* **2003**, *301*, 935 – 938.
[7] M. Valden, X. Lai, D. W. Goodman, *Science* **1998**, *281*, 1647 – 1650.
[8] N. Lopez, J. K. Nørskov, *J. Am. Chem. Soc.* **2002**, *124*, 11262 – 11263.
[9] M. S. Chen, D. W. Goodman, *Science* **2004**, *306*, 252 – 255.
[10] C. Lemire, R. Meyer, S. Shaikhutdinov, H. J. Freund, *Angew. Chem.* **2004**, *116*, 121 – 124; *Angew. Chem. Int. Ed.* **2004**, *43*, 118 – 121.
[11] V. A. Bondzie, S. C. Parker, C. T. Campbell, *Catal. Lett.* **1999**, *63*, 143 – 151.
[12] S. Carrettin, P. Concepción, A. Corma, J. M. López Nieto, V. F. Puntes, *Angew. Chem.* **2004**, *116*, 2592 – 2594; *Angew. Chem. Int. Ed.* **2004**, *43*, 2538 – 2540.
[13] G. C. Bond, D. T. Thompson, *Catal. Rev. Sci. Eng.* **1999**, *41*, 319 – 388.
[14] R. J. Davis, *Science* **2003**, *301*, 926 – 927.
[15] C. T. Campbell, *Science* **2004**, *306*, 234 – 235.
[16] J. Guzman, A. Corma, *Chem. Commun.* **2005**, *6*, 743 – 745.
[17] A. Corma, P. Atienzar, H. Garcia, J.-Y. Chane-Ching, *Nat. Mater.* **2004**, *3*, 394 – 397.
[18] A. M. Argo, J. F. Odzak, F. S. Lai, B. C. Gates, *Nature* **2002**, *415*, 623 – 626.
[19] These samples contained slightly larger gold clusters than those supported on the nanocrystalline support, with an average diameter of about 15 Å as indicated by the Au–Au first- and second-shell coordination numbers of 6 and 1 at interatomic distances of (2.8 ± 0.1) Å and (4.0 ± 0.1) Å, respectively. There are other supported metal samples with clusters almost as small as these for which the EXAFS metal–oxygen contributions are also negligible.[4,20]
[20] J. Guzman, B. C. Gates, *Nano Lett.* **2001**, *1*, 689 – 692.
[21] a) E. S. Putna, J. M. Vohs, R. J. Gorte, *J. Phys. Chem.* **1996**, *100*, 17862 – 17865; b) Q. Fu, A. Weber, M. Flytzani-Stephanopoulos, *Catal. Lett.* **2001**, *77*, 87 – 95; c) A. Boulahouache, G. Kons, H.-G. Lintz, P. Schulz, *Appl. Catal. A* **1992**, *91*, 115 – 123.
[22] V. V. Pushkarev, V. I. Kovalchuk, J. L. d'Itri, *J. Phys. Chem. B* **2004**, *108*, 5341 – 5348.
[23] R. Q. Long, Y. P. Huang, H. L. Wan, *J. Raman Spectrosc.* **1997**, *28*, 29 – 32.
[24] J. Guzman, S. Carrettin, A. Corma, *J. Am. Chem. Soc.* **2005**, *127*, 3286 – 3287.
[25] D. Andreeva, V. Idakiev, T. Tabakova, L. Ilieva, P. Falaras, A. Bourlinos, A. Travlos, *Catal. Today* **2002**, *72*, 51 – 57.

